

Water under extreme confinement in graphene: Oscillatory dynamics, structure, and hydration pressure explained as a function of the confinement width.

Carles Calero^{a,b}, Giancarlo Franzese^{a,b}

^a*Secció de Física Estadística i Interdisciplinària–Departament de Física de la Matèria
Condensada, Universitat de Barcelona, 08028 Barcelona, Spain*

^b*Institut de Nanociència i Nanotecnologia, Universitat de Barcelona, Barcelona, Spain*

Abstract

Graphene nanochannels are relevant for their possible applications, as in water purification, and for the challenge of understanding how they change the properties of confined liquids. Here, we use all-atom molecular dynamics simulations to investigate water confined in an open graphene slit-pore as a function of its width w , down to sub-nm scale. We find that the water translational and rotational dynamics exhibits an oscillatory dependence on w , due to water layering. The oscillations in dynamics correlate with those in hydration pressure, which can be negative (hydrophobic attraction), or as high as ~ 1 GPa, as seen in the experiments. At pore widths commensurable with full layers (around 7.0 Å and 9.5 Å for one and two layers, respectively), the free energy of the system has minima, and the hydration pressure vanishes. These are the separations at which the dynamics of confined water slows down. Nevertheless, the hydration pressure vanishes also where the free energy has maxima, i.e., for those pore-widths which are incommensurable with the formation of well-separated layers, as $w \simeq 8.0$ Å. Around these values of w , the dynamics is faster than in bulk, with water squeezed out from the pore. This behavior has not been observed for simple liquids under confinement, either for water in closed nano-pores. The decomposition of the free energy clarifies the origins of the dynamics speedups

Email addresses: carles.calero@ub.edu (Carles Calero), gfranzese@ub.edu (Giancarlo Franzese)

and slowdowns. In particular, we find that the nature of the slowdown depends on the number of water layers: for two layers, it is due to the internal energy contribution, as in simple liquids, while for one layer, it has an entropic origin possibly due to the existence of a hydrogen-bond network in water. Our results shed light on the mechanisms ruling the dynamics and thermodynamics of confined water and are a guide for future experiments.

Keywords: Water, Graphene, Confinement, Molecular Dynamics, Structure-Dynamics relation, Free energy

2010 MSC: 00-01, 99-00

1. Introduction

Experiments and theories show that liquids in strong confinement between solid boundaries exhibit very different dynamics and thermodynamics compared to the bulk [1, 2, 3, 4, 5, 6, 7, 8, 9, 10]. The interaction of fluids with the confining surface causes the structuring in layers of the liquid and affects its dynamics [11, 12, 13, 14, 15, 16, 17]. However, the experimental difficulties lead to debated results [18]. For example, a mobility of confined water higher than expected [19, 20, 21, 22, 18] is confirmed by several simulations of water [23, 24, 25, 22, 26, 27, 28], and of a water-like model [12], in nanotubes with a radius less than 1 nm. On the other hand, some simulations find that the diffusion coefficient of water in nanotubes simply decreases for decreasing confinement space down to 0.8 nm [29, 30], pointing at the relevance of the numerical limitations [31, 32, 8, 33].

Hydrated graphene interfaces are of particular interest due to possible applications, including desalination [34, 35, 36, 37, 38] decontamination [39, 40, 41], energy storage [42, 43], heterogeneous catalysis, graphene exfoliation and transferring [44, 16]. Graphene confinement enriches the complex phase diagram of bulk water in simulations [45, 46, 47, 48, 49, 50, 51, 52, 53, 4, 54, 55] and experiments [56, 57, 58, 59], and changes the water dynamics and structure, as seen numerically [60, 61, 62, 63, 8, 64, 65, 66, 5, 6, 67, 68, 69] and in laboratories [7, 70, 71].

Experiments in slit pores show that water forms layers parallel to the walls [72]. Computer simulations of water between two nanoscopic hydrophobic plates reveal that these layers correspond to local minima in the free-energy profile as a function of the plate-plate separation w [73] and that the water mobility in a hydrophobic slit pore monotonically increases as w becomes larger [74, 75, 76, 77, 78, 79, 80, 81, 82, 83]. Similar results hold for water confined in graphite [84] and quartz [45, 46, 76], with freezing of the dynamics at sub-nm confinement.

As the slit pore size w decreases, experiments and simulations show the emergence of oscillatory behavior in solvation forces and viscosity of water [9, 85, 55, 86]. This behavior is reminiscent of the oscillations in the diffusion constant and the free energy of a simple (Lennard-Jones) liquid confined in a slit-pore [87], and it calls into question a recent numerical work finding a plate-plate attraction that monotonically increases for decreasing w [88]. It is, therefore, unclear how strong (sub-nm) pore confinement affects water diffusion, hydration forces, and free energy, and which relation holds among them.

To contribute to this debate, here, we use all-atom molecular dynamics (MD) simulations to investigate the dynamical, structural, and thermodynamic properties of water confined between rigid graphene plates as a function of their separation, w , down to sub-nm size. To properly account for the most relevant conditions in which confined water is encountered in nature and in possible applications, we couple the confined system to a large reservoir of water molecules which are kept at constant temperature and pressure. We demonstrate that, under such conditions, the translational and rotational water dynamics have oscillatory dependence on the plate separation, and, through hydration-pressure and free-energy calculations, we show that such behavior directly correlates with structural properties of the confined water. The free-energy analysis allows us to clarify the origins of the dynamics speedups and slowdowns. In particular, we find that the slowdown mechanism depends on the number of water layers: it is due to the entropy when there is only one layer, while it is caused by the internal energy when the layers are two.

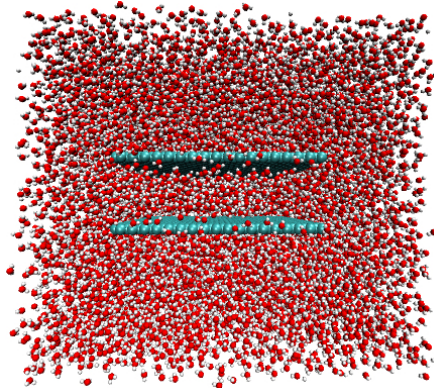


Figure 1: Our simulation box with two parallel graphene-plates surrounded by water. Carbon atoms are black, oxygen atoms red, and hydrogen atoms white. For clarity purposes, we do not show all the water molecules. The pore width w is the distance between the plates.

2. Methods

We simulate a system made of two $24.6 \text{ \AA} \times 25.5 \text{ \AA}$ rigid graphene-plates surrounded by water with periodic boundary conditions in the three spatial directions (Fig. 1). We consider fixed slit-pore widths $6 \leq w/\text{\AA} \leq 17$ and focus on the water molecules between the plates.

We use TIP4P/2005-water [89] and carbon atoms interacting through a Lennard-Jones potential with parameters from the CHARMM27 force field. We deduce the parameters of the water-carbon interaction adopting the Lorentz-Berthelot rules, and cut off the Van der Waals interactions at 12 \AA with a smooth switching function starting at 10 \AA . We compute the long-range electrostatic forces using the particle mesh Ewald method [90] with a grid space of $\approx 1 \text{ \AA}$. We use the GROMACS package [91] at constant temperature T and volume V , with 1 fs simulation time-step, and update the electrostatic interactions every 2 fs. If not indicated otherwise, we fix $T = 300 \text{ K}$ and, following other authors, e.g., [18, 46, 76, 92], we adopt a Berendsen thermostat [93] to control it.

Thermostating highly confined fluids has no perfect solution [94, 95, 96], and the Berendsen thermostat does not accurately reproduce the canonical fluctuations of temperature, which are relevant for thermodynamic properties, such as the specific heat. However, comparison of velocity rescaling, Berendsen, or Nosé-Hoover thermostats shows no effects on layering, diffusion, and the thermodynamic averages of confined water, which are the objects of our study [1, 97]. We fix the total volume of our simulation box to $V = 4.2 \times 4.2 \times 5.1 \text{ nm}^3$ and the total number of water molecules to $N = 2796$.

We prepare the initial configurations, corresponding to the different slit-pore width, with the help of the visualization software VMD [98]. First, we create the graphene layers and keep the positions of the carbon atoms frozen in the three spatial directions during the simulations. Then, we hydrate the system with TIP4P/2005 water molecules. We perform a short 1000-steps minimization run to avoid overlaps between molecules. Next, we simulate the system at constant N , V , and T , equilibrating for 5 ns. Then, we collect data every 10 ps for the next 50 ns and every 0.1 ps for the next 8 ns [91].

To avoid plates-boundaries effects, we analyze water molecules within the $A \times w$ central region between the plates, where $A = 15 \text{ \AA} \times 15 \text{ \AA}$. Because this confined sub-region is open and connected to a reservoir of water at constant N , V , and T , as it is the case of many experimental setups [7], the observables are calculated at constant chemical potential, μ , constant pressure P , and constant T . As we will discuss, allowing the density of the confined region to fluctuate leads to important differences with studies of similar confined systems simulated at a fixed density [61, 65].

3. Results and Discussion

3.1. Translational Dynamics

First, we study the dynamics –both translational and rotational– of water molecules confined between graphene plates at fixed w . To avoid biased sampling of the dynamics, we consider all water molecules within the central volume

$A \times w$ between the plates and collect their trajectories while they remain in the region. To improve statistics in the calculation of the evolution of the mean square displacement, we use multiple time origins.

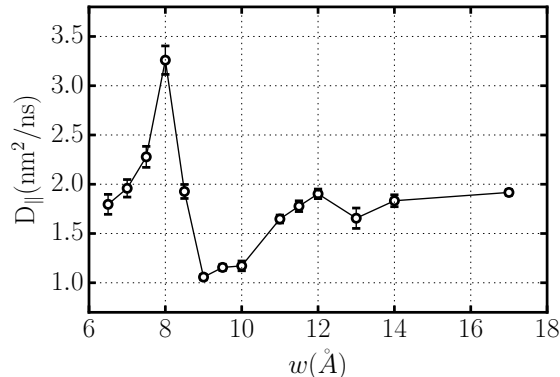


Figure 2: The confined-water diffusion coefficient D_{\parallel} , parallel to the plates, shows oscillatory behavior as a function of the plate separation w , with maxima at $w \simeq 8 \text{ \AA}$ and 12 \AA , and minima at $w \simeq 9 \text{ \AA}$ and 13 \AA

We find that D_{\parallel} , the diffusion coefficient of confined water along the directions parallel to the plates, exhibits oscillatory behavior as a function of w (Fig. 2). In particular, D_{\parallel} has two maxima and, at least, two minima for $6.5 \leq w/\text{\AA} \leq 17$, with the largest maximum, $\simeq 3.3 \text{ nm}^2/\text{ns}$, at $w \simeq 8 \text{ \AA}$ and the smallest value, $\simeq 1.0 \text{ nm}^2/\text{ns}$, at $w \simeq 9 \text{ \AA}$. For large w , and outside the confined region, the diffusion coefficient approaches the bulk value for TIP4P/2005-water, $\approx 2.1 \text{ nm}^2/\text{ns}$ at ambient conditions [89].

Hence, the translational diffusion of water in a slit-pore slows down, by a factor ≈ 0.5 for $w = 9 \text{ \AA}$, with respect to bulk water, while speeds up, by a factor ≈ 1.65 , when the confining distance is $w = 8 \text{ \AA}$, and finally decreases again for smaller values of w . The speedup is reminiscent of the debated [24, 8, 33] enhanced mobility of water in pores of a few nanometers [20, 19, 21, 22, 18], or at the water-vapor interface [99].

Also, we analyze the *survival probability*, i.e., the probability that a water

molecule spends a time t in the confined region, defined as

$$S^{(w)}(t) \equiv \left\langle \frac{N^{(w)}(t_0, t_0 + t)}{N^{(w)}(t_0)} \right\rangle, \quad (1)$$

where $N^{(w)}(t_0, t_0 + t)$ is the number of water molecules which remain in the confined region after a time t out of those that were in that region at t_0 , $N^{(w)}(t_0)$. The brackets $\langle \dots \rangle$ indicate average over different time origins t_0 .

We find that $S^{(w)}$ decays slowly and can be adjusted with a double exponential function, or a single exponential for $t > 1$ ps. The time τ_w at which $S^{(w)}(\tau_w) = 0.5$ is another property that characterizes the confined water, and its behavior (Fig. 3) confirms the oscillatory dependence of the translational dynamics as a function of the plate separation w , reaching minima where D_{\parallel} has maxima and *vice versa*¹.

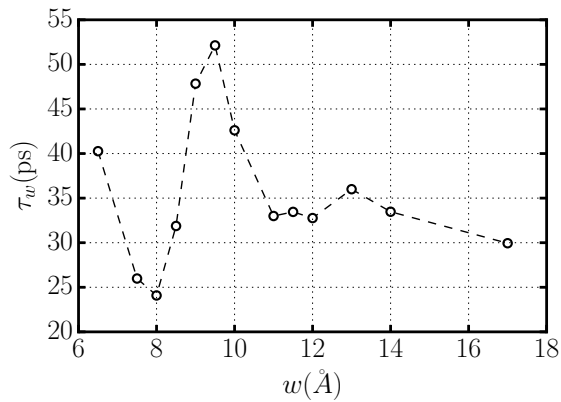


Figure 3: Characteristic time of water occupancy of the confined region τ_w as a function of the plate separation w .

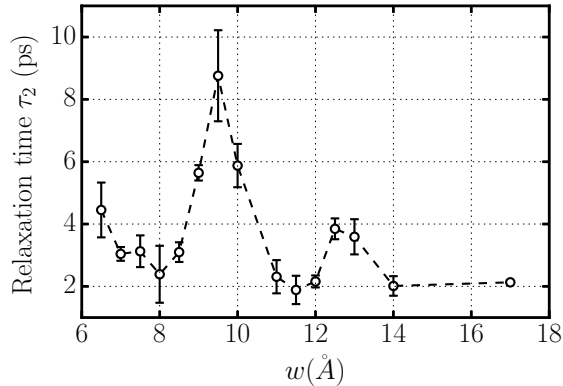


Figure 4: The reorientation correlation time τ_2 of confined water as a function of graphene-plate separation w is oscillatory with minima and maxima that correlates well with those of translational τ_w .

3.2. Rotational Dynamics

Next, we probe the effect of confinement on the rotational dynamics of water molecules by calculating the rotational dipolar correlation functions,

$$C_n(t) \equiv \langle P_n(\hat{\mu}(t) \cdot \hat{\mu}(0)) \rangle, \quad (2)$$

where $P_n(x)$ is the n -th order Legendre polynomial, $\hat{\mu}(t)$ is the direction of the water dipole vector at time t and $\langle \dots \rangle$ denote ensemble average over all water molecules and time origins. To quantify the relaxation of the correlation functions $C_n(t)$, we define the relaxation time

$$\tau_n \equiv \int_0^\infty C_n(t) dt, \quad (3)$$

which is not dependent on any assumptions on the functional form of the correlation function.

We find (Fig. 4) that for $w \geq 14$ Å the rotational dynamics of water molecules, characterized by the reorientation correlation time τ_2 , is $\tau_2 \approx (2.0 \pm$

¹The average thermal diffusion velocity along the main axis of the pore is of the order of 10^{-3} m/s, that is, as expected, at least two orders of magnitude smaller than the flow velocity of water under large pressure gradients (1 PPa/m) through graphene nanocapillaries [18].

0.2)ps, consistent with values for bulk TIP4P/2005-water at $T = 300$ K [100]. For $w < 14$ Å, also τ_2 exhibits an oscillatory dependence on the distance w . It has, at least, two maxima, reaching a value ($\approx 8.5 \pm 1.5$)ps, i.e., ≈ 4.25 times larger than bulk, at $w \simeq 9.5$ Å. It decreases to the bulk value for $w \simeq 8$ Å, and finally increases again for smaller separations. The maxima and minima of τ_2 correlate well with those of the translational τ_w and the oscillatory behavior of $D_{||}$, suggesting a coupling of translation and orientation dynamics in confined water under the thermodynamic conditions considered here, and consistent with the existence of cooperative rearranging regions due to the water hydrogen bonds [101].

3.3. Structure

For all the plate separations we considered here, we find that the confined water remains in the liquid phase and organizes into layers parallel to the confining walls at well defined values of w : one layer for $6.5 \leq w/\text{Å} \leq 7.0$, two for $9.0 < w/\text{Å} < 10.0$, three for $12.5 < w/\text{Å} < 14.0$ (Fig. 5). These results are consistent with previous works performed under similar conditions [86]^{2 3}.

As a result of the formation of layers, the slit-pore *acceptance capacity* per unit area $\sigma \equiv N(w)/A$ does not depend linearly with plate separation w but exhibits a steplike pattern (Fig. 6a), consistent with previous results [86], as emphasized by plotting the derivative $d\sigma/dw$ (Fig. 6b). Here, $N(w)$ is the number of water molecules confined in the central region $A \times w$ and is calculated by integrating the density profiles at each w . The derivative $d\sigma/dw$ is a measure

²At pore width 9 Å, we find a peak height for the density profile that is approximate twice the values in Ref.s [61] and [65]. This apparent discrepancy occurs because these Ref.s adopt the constant- NVT ensemble, while we use the constant- μPT ensemble, as in Ref. [86]. Also, this observation is supported by the results in Ref. [102], where the authors find the same peak height for Lennard-Jones particles with size 3.405 Å, comparable to a water molecule, in a slit-pore with 9 Å width, simulated at constant- μPT in a geometry similar to the one we adopt here.

³Layering occurs at any interface, including at liquid-vapor interfaces once the smearing effect of the capillary waves is removed [99]

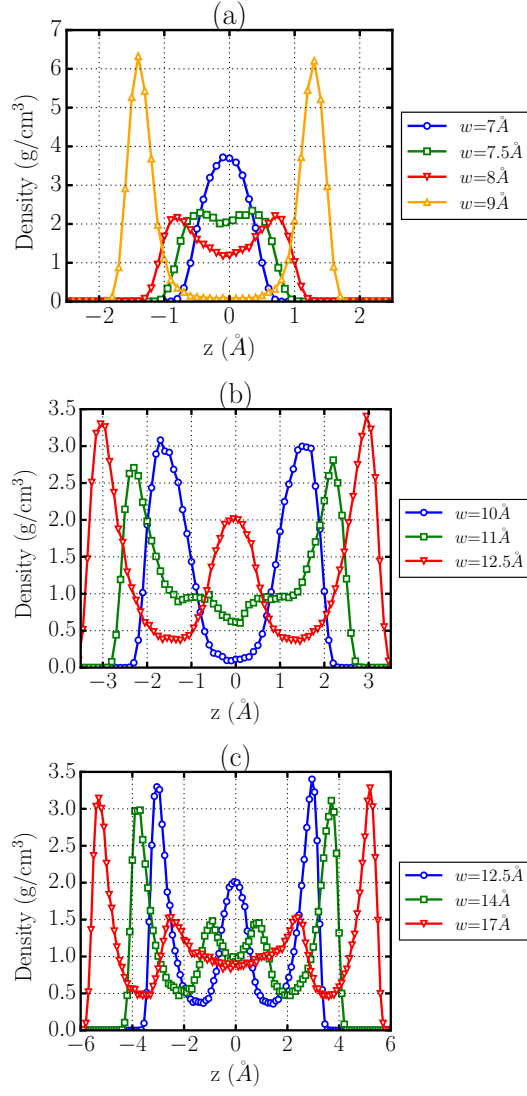


Figure 5: Water density-profile as a function of the distance z from the center of the slit-pore, for different values of graphene-plate distance w . We find: (a) from one to two layers for $7.0 < w/\text{\AA} \leq 9.0$, (b) from two to three layers for $10.0 < w/\text{\AA} \leq 12.5$, (c) from three to four layers for $12.5 < w/\text{\AA} \leq 17.0$.

of the variation of the acceptance capacity of the slit-pore upon changing w and exhibits a non-monotonic behavior, as expected due to the layering. Minima in

$d\sigma/dw$ occur at values of w at which full layers are present. Maxima in $d\sigma/dw$, instead, occur for those values of w such that a new layer is forming.

We observe that the non-monotonic behavior of $d\sigma/dw$ shows a clear correlation with the dependence of confined water dynamics with plate separation w . Indeed, both translational (Fig. 2) and rotational (Fig. 4) water dynamics are faster when $d\sigma/dw$ is larger, and become slower when $d\sigma/dw$ decreases. Our observation corroborates the conclusion from experiments showing a flow enhancement in channels with only a few layers of water, that the authors associate with an increased structural order in nanoconfined water [18].

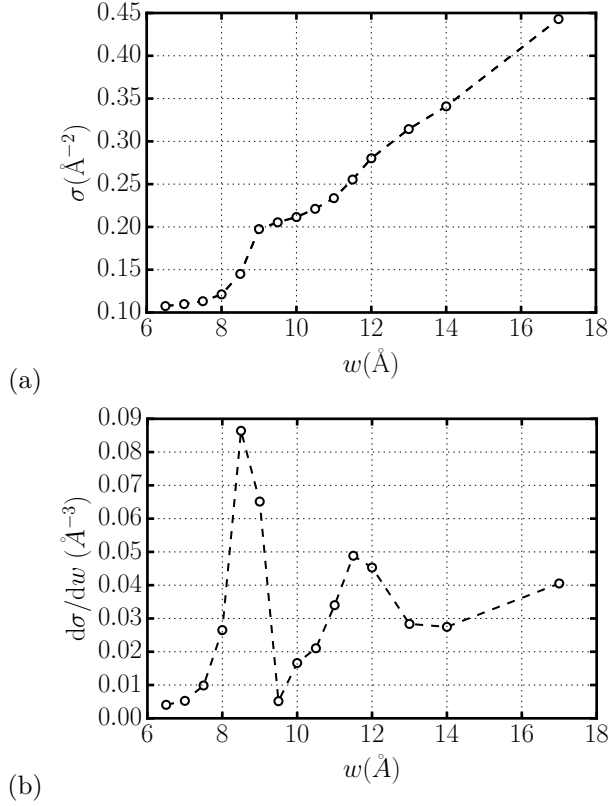


Figure 6: The slit-pore acceptance capacity per unit area σ and its derivative as a function of graphene-plate separation w . (a) σ increases monotonically with w , but at different rates depending on w . (b) The derivative $d\sigma/dw$ is non-monotonic, with maxima and minima. The derivative reaches values close to zero at $w \approx 7.0 \text{ \AA}$ and 9.5 \AA .

3.4. Hydration pressure

To understand the relation of the dynamics with the thermodynamics, we calculate the *hydration pressure*, i.e., the pressure exerted by confined water perpendicularly to the graphene plates, defined as

$$\Pi \equiv p_{\text{in}}^{\perp} - p_{\text{out}}^{\perp}, \quad (4)$$

where p_{in}^{\perp} and p_{out}^{\perp} are the internal and, respectively, external pressures of water in the direction perpendicular to the plates, calculated as the vectorial sum over all the forces due to water acting on the plates, divided by the section (surface) of the plates [103, 46].

We calculate Π for each specific values of w and for two different temperatures, 300 K and 275 K (Fig. 7). Due to the relatively small size of the confined region with respect to the simulated system, the external pressure p_{out}^{\perp} is insensitive to the change in the slit-pore width w and is given by $p_{\text{out}}^{\perp} = (400 \pm 100)$ bar.

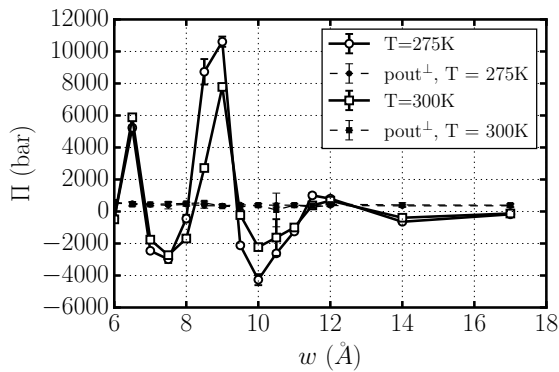


Figure 7: Average pressures as a function of graphene-plate separation w at $T = 300$ K (squares) and 275 K (circles). In both cases, the hydration pressures Π (continuous lines) are non-monotonic, while the external pressures (dashed lines) are constant. The external pressure $p_{\text{out}}^{\perp} = (400 \pm 100)$ bar is constant with respect to w . Where not visible, the error bars are smaller than the symbols' size.

We find that Π oscillates between positive and negative values. The values of w at which the Π minima and maxima occur do not display evident depen-

dence on T [86] and are at distances separated by approximately the molecular diameter of the water molecule. Minima and maxima follow a pattern that resembles that of dynamical quantities (Figs. 2, 3, 4) and the acceptance capacity variation (Fig. 6) with w , but do not coincide.

In particular, we observe that it is $\Pi \approx 0$ at values that are close to those at which D_{\parallel} , τ_w , τ_2 and $d\sigma/dw$ have local maxima or minima. Comparison with the water density-profile (Fig. 5) clarifies that some of the values of w at which $\Pi \approx 0$ correspond to those for optimal layer-wall, and layer-layer, separations. For example, at $T = 300$ K this value is $6.5 < w/\text{\AA} < 7.0$ for one layer, for two layers is $9.0 < w/\text{\AA} < 10.0$. However, Π vanishes also at intermediate values of w , which are, as we will discuss next, related to marginally-stable configurations.

At intermediate values of w , the amount of confined water could be above or below the number that optimizes the inter-layers distance, causing repulsion ($\Pi > 0$) or attraction ($\Pi < 0$), respectively, between the plates. In these cases, an external constraint on the plates' position provides the mechanical stability along the direction perpendicular to the slit-pore.

At $T = 300$ K, the necessary external pressure to keep the plates at a fixed distance is ≈ 0.6 GPa for $w = 6.5$ \AA, a width smaller than the optimal value for one confined water monolayer, and ≈ 0.8 GPa for at $w = 9$ \AA, which is just below the optimal value for two layers. Instead, the walls effectively attract each other (with ≈ -0.3 GPa for $w = 7.5$ \AA, and ≈ -0.2 GPa for 10.0 \AA) for w above the optimal distance for one or two water layers.

Lowering T at 275 K, the effective plate-plate attraction increases to ≈ -0.4 GPa for $w = 10.0$ \AA, and the repulsive pressure increases to ≈ 1.1 GPa for $w = 9$ \AA. This large variation of Π at $T = 275$ K is due to the energy change associated to the reentrant crystallization into a bilayer hexagonal ice for $9.0 < w/\text{\AA} < 9.5$ [5], that is larger than the energy change for restructuring liquid water at $T = 300$ K. These results are consistent, for order of magnitude, with the capillary pressure estimated in simulations of graphene pores that accommodate two layers of water (≈ 1 GPa at $\simeq 9$ \AA) [56, 104].

Hence, our calculations confirm that (i) water-mediated plate-plate forces

oscillate [86, 55], at variance with Ref. [88]; (ii) the oscillations correlate with large structural changes of the solvent, e.g., the layers merging or the ice melting. Furthermore, we clarify that the water dynamics oscillates as well, with speedups or slowdowns, with respect to bulk water, associated to these large pressures changes. To better understand the thermodynamic nature of these dynamic changes, we analyze next the free energy of the confined water.

3.5. Free energy

Following Gao et al. [87, 102], we calculate the free-energy variation per confined water molecule, $\Delta f(w)$, as the work done against the hydration forces to approach the two graphene plates from our largest separation, $w_0 = 17 \text{ \AA}$, to any smaller w , where

$$\Delta f(w) \equiv \Delta f(w_0 \rightarrow w) \equiv f(w) - f(w_0) \equiv - \int_{w_0}^w \mathfrak{f}_{\text{hyd}}^\perp(w') dw', \quad (5)$$

and $\mathfrak{f}_{\text{hyd}}^\perp(w) \equiv \Pi(w)/\sigma(w)$ is the hydration force, per confined water molecule, acting on the plates at separation w (Fig. 8).

Our calculation of $\Delta f(w)$ clarifies that the work per molecule necessary to approach the two confining surfaces is non-monotonic with w , as well as all the other dynamic, structural and thermodynamic quantities we presented here. In particular, the work oscillates depending on how strong is the water-mediated effective interaction between the walls, with extrema in $\Delta f(w)$ correlated to the zeros of Π , with minima and maxima in $\Delta f(w)$ corresponding to stable and marginally-stable configurations, respectively.

The negative values of $\Delta f(w)$ show that the confined system gains energy at the w of the minima. In particular, the work per molecule has its absolute minimum, $\Delta f(w) \approx -3.0 \text{ kJ/mol}$, at $w \approx 9.5 \text{ \AA}$, i.e., when there are two layers of confined water (Fig. 5a). Another strong minimum, $\Delta f(w) \approx -1.8 \text{ kJ/mol}$, occurs at $w \approx 7.0 \text{ \AA}$, corresponding to one single layer of confined water, while the minimum, $\Delta f(w) \approx -0.6 \text{ kJ/mol}$, at $w \approx 13.0 \text{ \AA}$, with three confined layers, is weaker. These results, showing that nanoconfined water forms

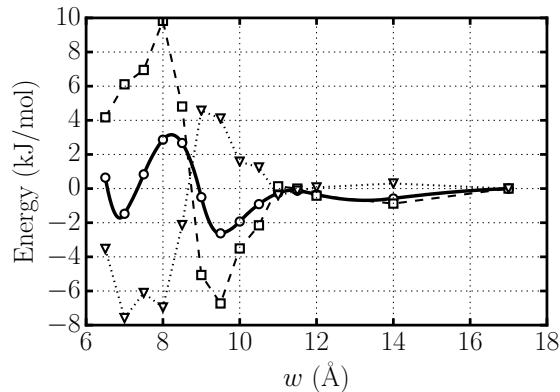


Figure 8: Work per confined water molecule performed to approach the graphene plates from $w_0 = 17 \text{ \AA}$ to w , $\Delta f(w)$ (solid line with circles), as a function of the separation w at $T = 300 \text{ K}$. This work has two contributions: the internal energy part (dashed line with squares) and the entropic part (dotted line with with triangles). The minimum of $\Delta f(w)$ at $w \approx 9.5 \text{ \AA}$ (water bilayer) corresponds to a minimum in internal (attractive) energy $\Delta u(w)$ per water molecule, while the minimum at $w \approx 7.0 \text{ \AA}$ (water monolayer) to a minimum in the entropy term (disordering) $-T\Delta s_{in}$ per water molecule, despite the positive internal (repulsive) energy.

preferentially monolayers and bilayers, are consistent with experiments under similar conditions [105, 57, 106] and recent simulations[86].

To understand the nature of minima we calculate the separate component of the free energy. First, we observe that Eq. (5) corresponds to the Helmholtz free energy of confined water in a volume with a constant number of water molecules [87, 102]. Hence, $\Delta f \equiv \Delta f_{in} = \Delta u_{in} - T\Delta s_{in}$, where $\Delta u_{in} \equiv u_{in}(w) - u_{in}(w_0)$ is the internal energy change per confined water molecule, and $\Delta s_{in} \equiv s_{in}(w) - s_{in}(w_0)$ is the corresponding entropy change per confined water molecule. Because in our system $N(w) \ll N$, and the water outside the pore is, in first approximation, not affected by the change in w , we approximate $\Delta u_{in} \approx \Delta u$ of the entire system, simplifying the calculation for the long-range electrostatic interaction (requiring periodic boundary conditions for the Ewald summation).

Knowing Δf and Δu , we estimate $-T\Delta s_{in}$ as their difference (Fig. 8). We

find that the nature of the two free-energy minima for water bilayer and monolayer are quite different.

The free-energy minimum at $w \approx 9.5 \text{ \AA}$ (water bilayer) is dominated by the internal energy contribution $\Delta u < 0$ among the water molecules, inducing an effective attractive force between the walls for $9.5 \leq w/\text{\AA} \leq 11.5$, and an effective repulsion for $8.0 < w/\text{\AA} < 9.5$ (Fig.7). The entropy term $-T\Delta s_{\text{in}} > 0$ is associated with an increase of order in the confined water bilayer with respect to the multilayers at w_0 . This is similar to what has been found in confined Lennard-Jones liquids [87].

The free-energy minimum at $w \approx 7.0 \text{ \AA}$ (water monolayer) is dominated, instead, by the entropy contribution $-T\Delta s_{\text{in}}$, i.e., the monolayer has a structure that is more disordered than the water multilayer. Furthermore, the internal energy $\Delta u > 0$ among the water molecules is overall repulsive. Despite this repulsion, the effective force between the walls is attractive for $7.0 \leq w/\text{\AA} \leq 8.0$ and repulsive for $6.0 < w/\text{\AA} < 7.0$ (Fig.7). This effect could be a consequence of the hydrogen bond interactions among water molecules. The strong confinement, indeed, induces a deformation of the hydrogen bonds [45, 56], increasing both the energy of the configurations ($\Delta u > 0$) and their degeneracy ($\Delta s_{\text{in}} > 0$).

The two free-energy minima are separated by a maximum, $\Delta f(w) \approx 3.0$ kJ/mol, at $w \approx 8 \text{ \AA}$. This free-energy barrier is due to the combination of the stronger water-water repulsion ($\Delta u > 0$) and the disordering effect ($\Delta s_{\text{in}} > 0$) associated with the expulsion of water from the pore (Fig.5), and its value, ≈ 5.0 kJ/mol, is twice as large as the thermal energy per mole at $T = 300 \text{ K}$.

4. Summary and Conclusions

We study the dynamics and thermodynamics of water confined between two graphene walls at distance w , down to the sub-nm scale. Our molecular dynamics simulations show that all the calculated quantities have oscillatory dependence on w due to layering.

We focus on the translational and rotational dynamics. We find that (i) the

diffusion constant D_{\parallel} parallel to the confining walls, (ii) the characteristic time τ_w of occupancy of the pore, and (iii) the reorientation correlation time τ_2 of confined water oscillate, as a function of the plate separation w , and correlate among them.

The overall dynamics slows down at pore widths commensurable with three, one, and, in particular, two full layers. It speeds up, instead, at pore widths that are incommensurable with full layers, with a surprisingly large factor at sizes between a bilayer and a monolayer. Squeezing the pore around 8 Å, considerably increases the thermal diffusion of the confined water, supporting the enhanced mobility seen in experiments with carbon nanotubes, membranes, and capillaries with nm-sized pores [20, 19, 21, 22, 18].

To the best of our knowledge, this oscillatory sequence of repeated minima and maxima for translational and rotational dynamics of water, in a graphene slit pore as a function of the plate separation, has not been reported so far. Consistent numerical results by Neek-Amal et al. [85] show oscillatory shear viscosity of water between two parallel graphene layers, separated by less than 2 nm. As in our analysis, the oscillations originate from the commensurability between the capillary size and the size of water molecules. If the Stokes-Einstein (SE) relation were valid in extreme confinement, the D_{\parallel} oscillation would be related to those of the viscosity. However, Köhler et al. [107] show that the SE relation breaks in narrow (with diameters less than 4.07 nm) hydrophobic nanotubes, questioning the validity of the SE also in hydrophobic slit-pores, and, as a consequence, the possible relation between shear viscosity and diffusion coefficient in nm-size graphene confinement.

On the other hand, previous results for Lennard-Jones particles in a slit-pore, with particle sizes comparable to water molecules, display a diffusion constant that oscillates below confining distances of 2 nm [87]. As in our case, Gao et al. relate this behavior to oscillating hydration forces and oscillating free energy. However, differently from our case, they find no dynamics speedup in confinement with respect to the bulk. The fast diffusion and rotation dynamics in very narrow pores could be, therefore, a peculiar property of water, that we

can explain in terms of hydration forces and free energy.

In particular, our free energy analysis elucidates the origin of the water behavior in sub-nm confinement. When the water bilayer forms at $w \approx 9.5 \text{ \AA}$, the water-water overall attraction, and the structural ordering, generate a free-energy minimum that slows down the dynamics. At the pore width for a full bilayer, the hydration pressure is zero, and there is no need for external forces to reach mechanical stability.

By reducing w , water repulsion and structural disorder take over. At $w \approx 8.0 \text{ \AA}$, it is necessary to apply high external pressure (of the order of $\approx 1 \text{ GPa}$) to reach mechanical stability for the confined water, and the water dynamics largely speeds up.

Below $w \approx 8.0 \text{ \AA}$, the wall-wall effective interaction is again attractive and the system collapses toward the width $w \approx 7.0 \text{ \AA}$, corresponding to the free-energy minimum for a confined monolayer. At the same time, the dynamics slows down to the bulk value approximately. The origin of the monolayer free-energy minimum is, however, quite different from the bilayer case. It is the increase of entropy of the monolayer, with respect to bulk, that generates the minimum, while the overall water-water interaction is repulsive at this confinement. We suggest that this result could be an effect of *a*) the distortion of the water hydrogen bonds and *b*) the consequent large degeneracy within water configurations with the same internal energy.

Consistent with experimental observations, we find that the bilayer at $w = 9.5 \text{ \AA}$ is more stable than the monolayer at $\approx 7.0 \text{ \AA}$ [57, 105, 106] and that the transformation from bilayer to monolayer requires an energy that is twice as large as the thermal energy per mole at $T = 300 \text{ K}$. The same transformation is associated to a reentrant crystallization into a bilayer hexagonal ice at $T = 275 \text{ K}$.

We find that, within this sub-nm range of pore widths, the hydration-pressure oscillations are much stronger than at larger pore sizes. This result clarifies that the apparent contradiction between recent numerical works, with [55, 86] or without oscillations [88] in the water-mediated wall-wall interaction,

is possibly due to a lack of resolution in the sub-nm range of the pore size. Furthermore, we expect increases in the compressibility of the confined water at those pore widths at which the hydration pressure is zero but the system is mechanically marginally-stable, i.e., near the free-energy maxima at $8 \leq w/\text{\AA} \lesssim 8.5$ and $w \approx 11.5 \text{\AA}$, consistent with Ref. [86].

In conclusion, our results provide a thermodynamically consistent account of recent experimental observations for water confined in graphene slit pores, or similar confinements. They shed light on the origin of oscillations of the hydration force under sub-nanometer confinement from a structural and a thermodynamical perspective, resolving apparent contradictions in recent results. Furthermore, our results reveal, for the first time, the oscillatory behavior of the dynamical properties of confined water on the same scale. We suggest that the nature of such oscillations is a unique feature of sub-nm confined water, supporting further studies for possible applications.

5. Acknowledgments

We thank Fabio Leoni and Jordi Martí for useful discussions. We acknowledge the support of Spanish grant PGC2018-099277-B-C22 (MCIU/AEI/ERDF). CC acknowledges the support from the Catalan Governament Beatriu de Pinós program (BP-DGR 2011). GF acknowledges the support by ICREA Foundation (ICREA Academia prize). This work was partially funded by Horizon 2020 program through 766972-FET-OPEN-NANOPHLOW. The authors thankfully acknowledges the computer resources, technical expertise and assistance provided by the Red Española de Supercomputación.

References

References

- [1] P. Loche, C. Ayaz, A. Wolde-Kidan, A. Schlaich, R. R. Netz, Universal and nonuniversal aspects of electrostatics in aqueous nanoconfinement,

The Journal of Physical Chemistry B 124 (21) (2020) 4365–4371. doi:
10.1021/acs.jpcc.0c01967.

URL <https://doi.org/10.1021/acs.jpcc.0c01967>

- [2] A. W. Knight, N. G. Kalugin, E. Coker, A. G. Ilgen, Water properties under nano-scale confinement, *Scientific Reports* 9 (1) (2019) 8246. doi:
10.1038/s41598-019-44651-z.

URL <https://doi.org/10.1038/s41598-019-44651-z>

- [3] L. Fumagalli, A. Esfandiari, R. Fabregas, S. Hu, P. Ares, A. Janardanan, Q. Yang, B. Radha, T. Taniguchi, K. Watanabe, G. Gomila, K. S. Novoselov, A. K. Geim, Anomalously low dielectric constant of confined water, *Science* 360 (6395) (2018) 1339.

URL <http://science.sciencemag.org/content/360/6395/1339.abstract>

- [4] Z. Gao, N. Giovambattista, O. Sahin, Phase diagram of water confined by graphene, *Scientific Reports* 8 (1) (2018) 6228. doi:10.1038/s41598-018-24358-3.

URL <https://doi.org/10.1038/s41598-018-24358-3>

- [5] J. Martí, C. Calero, G. Franzese, Structure and dynamics of water at carbon-based interfaces, *Entropy* 19 (3) (2017) 135. doi:10.3390/e19030135.

URL <http://www.mdpi.com/1099-4300/19/3/135>

- [6] L. Yang, Y. Guo, D. Diao, Structure and dynamics of water confined in a graphene nanochannel under gigapascal high pressure: dependence of friction on pressure and confinement, *Phys. Chem. Chem. Phys.* 19 (2017) 14048–14054. doi:10.1039/C7CP01962A.

URL <http://dx.doi.org/10.1039/C7CP01962A>

- [7] R. R. Nair, H. A. Wu, P. N. Jayaram, I. V. Grigorieva, A. K. Geim, Unimpeded permeation of water through helium-leak-tight graphene-based

membranes, *Science* 335 (6067) (2012) 442–444.

URL <http://www.sciencemag.org/content/335/6067/442.abstract>

- [8] K. Falk, F. Sedlmeier, L. Joly, R. R. Netz, L. Bocquet, Molecular origin of fast water transport in carbon nanotube membranes: Superlubricity versus curvature dependent friction, *Nano Letters* 10 (10) (2010) 4067–4073. doi:10.1021/nl1021046.

URL <http://dx.doi.org/10.1021/nl1021046>

- [9] A. Verdaguer, G. M. Sacha, H. Bluhm, M. Salmeron, Molecular structure of water at interfaces: Wetting at the nanometer scale, *Chemical Reviews* 106 (4) (2006) 1478–1510. doi:10.1021/cr0403761.

URL <http://dx.doi.org/10.1021/cr0403761>

- [10] K. Koga, H. Tanaka, X. C. Zeng, First-order transition in confined water between high-density liquid and low-density amorphous phases, *Nature* 408 (6812) (2000) 564–567.

URL <http://dx.doi.org/10.1038/35046035>

- [11] J. Slovák, K. Koga, H. Tanaka, X. C. Zeng, Confined water in hydrophobic nanopores: Dynamics of freezing into bilayer ice, *Physical Review E* 60 (5) (1999) 5833–5840.

URL <http://link.aps.org/doi/10.1103/PhysRevE.60.5833>

- [12] J. R. Bordin, A. B. de Oliveira, A. Diehl, M. C. Barbosa, Diffusion enhancement in core-softened fluid confined in nanotubes, *The Journal of Chemical Physics* 137 (8) (2012) 084504–7.

URL <http://dx.doi.org/10.1063/1.4746748>

- [13] L. B. Krott, M. C. Barbosa, Anomalies in a waterlike model confined between plates, *The Journal of Chemical Physics* 138 (8) (2013) 084505–12.

URL <http://dx.doi.org/10.1063/1.4792639>

- [14] F. Leoni, G. Franzese, Structural behavior and dynamics of an anomalous fluid between attractive and repulsive walls: Templating, molding, and superdiffusion, *The Journal of Chemical Physics* 141 (17) (2014) 174501. doi:<http://dx.doi.org/10.1063/1.4899256>.
URL <http://scitation.aip.org/content/aip/journal/jcp/141/17/10.1063/1.4899256>
- [15] F. Leoni, G. Franzese, Effects of confinement between attractive and repulsive walls on the thermodynamics of an anomalous fluid, *Physical Review E* 94 (6) (2016) 062604–. URL <http://link.aps.org/doi/10.1103/PhysRevE.94.062604>
- [16] P. Bampoulis, K. Sotthewes, E. Dollekamp, B. Poelsema, Water confined in two-dimensions: Fundamentals and applications, *Surface Science Reports* 73 (6) (2018) 233–264. doi:<https://doi.org/10.1016/j.surfrep.2018.09.001>.
URL <http://www.sciencedirect.com/science/article/pii/S016757291830044X>
- [17] I. N. Tsimpanogiannis, O. A. Moulτος, L. F. M. Franco, M. B. d. M. Spera, M. Erdős, I. G. Economou, Self-diffusion coefficient of bulk and confined water: a critical review of classical molecular simulation studies, *Molecular Simulation* 45 (4-5) (2019) 425–453. doi:[10.1080/08927022.2018.1511903](https://doi.org/10.1080/08927022.2018.1511903).
URL <https://doi.org/10.1080/08927022.2018.1511903>
- [18] B. Radha, A. Esfandiar, F. C. Wang, A. P. Rooney, K. Gopinadhan, A. Keerthi, A. Mishchenko, A. Janardanan, P. Blake, L. Fumagalli, M. Lozada-Hidalgo, S. Garaj, S. J. Haigh, I. V. Grigorieva, H. A. Wu, A. K. Geim, Molecular transport through capillaries made with atomic-scale precision, *Nature* 538 (7624) (2016) 222–225.
URL <http://dx.doi.org/10.1038/nature19363>

- [19] M. Majumder, N. Chopra, R. Andrews, B. J. Hinds, Nanoscale hydrodynamics: Enhanced flow in carbon nanotubes, *Nature* 438 (7064) (2005) 44.
URL <http://dx.doi.org/10.1038/43844a>
- [20] J. K. Holt, H. G. Park, Y. Wang, M. Stadermann, A. B. Artyukhin, C. P. Grigoropoulos, A. Noy, O. Bakajin, Fast mass transport through sub-2-nanometer carbon nanotubes, *Science* 312 (5776) (2006) 1034–1037.
- [21] M. Majumder, N. Chopra, B. J. Hinds, Mass transport through carbon nanotube membranes in three different regimes: Ionic diffusion and gas and liquid flow, *ACS Nano* 5 (5) (2011) 3867–3877. doi:10.1021/nl200222g.
URL <http://dx.doi.org/10.1021/nl200222g>
- [22] X. Qin, Q. Yuan, Y. Zhao, S. Xie, Z. Liu, Measurement of the rate of water translocation through carbon nanotubes, *Nano Letters* 11 (5) (2011) 2173–2177. doi:10.1021/nl200843g.
URL <http://dx.doi.org/10.1021/nl200843g>
- [23] R. J. Mashl, S. Joseph, N. R. Aluru, E. Jakobsson, Anomalously immobilized water: A new water phase induced by confinement in nanotubes, *Nano Letters* 3 (5) (2003) 589–592. doi:10.1021/nl10340226.
URL <http://dx.doi.org/10.1021/nl10340226>
- [24] J. A. Thomas, A. J. H. McGaughey, Reassessing fast water transport through carbon nanotubes, *Nano Letters* 8 (9) (2008) 2788–2793. doi:10.1021/nl18013617.
URL <http://dx.doi.org/10.1021/nl18013617>
- [25] J. A. Thomas, A. J. H. McGaughey, Water flow in carbon nanotubes: Transition to subcontinuum transport, *Physical Review Letters* 102 (18) (2009) 184502–.
URL <http://link.aps.org/doi/10.1103/PhysRevLett.102.184502>

- [26] H. Ye, H. Zhang, Y. Zheng, Z. Zhang, Nanoconfinement induced anomalous water diffusion inside carbon nanotubes, *Microfluidics and Nanofluidics* 10 (6) (2011) 1359–1364. doi:10.1007/s10404-011-0772-y.
URL <http://dx.doi.org/10.1007/s10404-011-0772-y>
- [27] A. Barati Farimani, N. R. Aluru, Spatial diffusion of water in carbon nanotubes: From fickian to ballistic motion, *The Journal of Physical Chemistry B* 115 (42) (2011) 12145–12149. doi:10.1021/jp205877b.
URL <http://dx.doi.org/10.1021/jp205877b>
- [28] Y.-g. Zheng, H.-f. Ye, Z.-q. Zhang, H.-w. Zhang, Water diffusion inside carbon nanotubes: mutual effects of surface and confinement, *Physical Chemistry Chemical Physics* 14 (2) (2012) 964–971.
URL <http://dx.doi.org/10.1039/C1CP22622C>
- [29] Y.-C. Liu, J.-W. Shen, K. E. Gubbins, J. D. Moore, T. Wu, Q. Wang, Diffusion dynamics of water controlled by topology of potential energy surface inside carbon nanotubes, *Physical Review B* 77 (12) (2008) 125438–.
URL <http://link.aps.org/doi/10.1103/PhysRevB.77.125438>
- [30] T. Nanok, N. Artrith, P. Pantu, P. A. Bopp, J. Limtrakul, Structure and dynamics of water confined in single-wall nanotubes, *The Journal of Physical Chemistry A* 113 (10) (2008) 2103–2108. doi:10.1021/jp8088676.
URL <http://dx.doi.org/10.1021/jp8088676>
- [31] Y. Liu, Q. Wang, T. Wu, L. Zhang, Fluid structure and transport properties of water inside carbon nanotubes, *The Journal of Chemical Physics* 123 (23) (2005) 234701–7.
URL <http://link.aip.org/link/?JCP/123/234701/1>
- [32] B. Mukherjee, P. K. Maiti, C. Dasgupta, A. K. Sood, Strong correlations and fickian water diffusion in narrow carbon nanotubes, *The Journal of Chemical Physics* 126 (12) (2007) 124704–8.
URL <http://dx.doi.org/10.1063/1.2565806>

- [33] S. K. Kannam, B. D. Todd, J. S. Hansen, P. J. Daivis, How fast does water flow in carbon nanotubes?, *The Journal of Chemical Physics* 138 (9) (2013) 094701. doi:10.1063/1.4793396.
URL <https://doi.org/10.1063/1.4793396>
- [34] T. Humplik, J. Lee, S. C. O'Hern, B. A. Fellman, M. A. Baig, S. F. Hassan, M. A. Atieh, F. Rahman, T. Laoui, R. Karnik, E. N. Wang, Nanostructured materials for water desalination, *Nanotechnology* 22 (29) (2011) 292001.
URL <http://stacks.iop.org/0957-4484/22/i=29/a=292001>
- [35] D. Cohen-Tanugi, J. C. Grossman, Water desalination across nanoporous graphene, *Nano Letters* 12 (7) (2012) 3602–3608. doi:10.1021/nl3012853.
URL <http://dx.doi.org/10.1021/nl3012853>
- [36] S. C. O'Hern, M. S. H. Boutilier, J.-C. Idrobo, Y. Song, J. Kong, T. Laoui, M. Atieh, R. Karnik, Selective ionic transport through tunable sub-nanometer pores in single-layer graphene membranes, *Nano Letters* 14 (3) (2014) 1234–1241. doi:10.1021/nl404118f.
URL <http://dx.doi.org/10.1021/nl404118f>
- [37] G. P. Thiel, Salty solutions, *Physics Today* 68 (6) (2015) 66.
- [38] M. H. Köhler, J. Bordin, M. C. Barbosa, Ion flocculation in water: From bulk to nanoporous membrane desalination, *Journal of Molecular Liquids* doi:<https://doi.org/10.1016/j.molliq.2018.12.077>.
URL <http://www.sciencedirect.com/science/article/pii/S0167732218340728>
- [39] A. Y. Romanchuk, A. S. Slesarev, S. N. Kalmykov, D. V. Kosynkin, J. M. Tour, Graphene oxide for effective radionuclide removal, *Physical Chemistry Chemical Physics* (2013) –.
URL <http://dx.doi.org/10.1039/C2CP44593J>

- [40] S. Vadahanambi, S.-H. Lee, W.-J. Kim, I.-K. Oh, Arsenic removal from contaminated water using three-dimensional graphene-carbon nanotube-iron oxide nanostructures, *Environmental Science & Technology* 47 (18) (2013) 10510–10517. doi:10.1021/es401389g.
URL <http://dx.doi.org/10.1021/es401389g>
- [41] L. Xu, J. Wang, The application of graphene-based materials for the removal of heavy metals and radionuclides from water and wastewater, *Critical Reviews in Environmental Science and Technology* 47 (12) (2017) 1042–1105. doi:10.1080/10643389.2017.1342514.
URL <https://doi.org/10.1080/10643389.2017.1342514>
- [42] Z. Bo, H. Yang, S. Zhang, J. Yang, J. Yan, K. Cen, Molecular insights into aqueous nacl electrolytes confined within vertically-oriented graphenes, *Scientific Reports* 5 (2015) 14652 EP –.
URL <http://dx.doi.org/10.1038/srep14652>
- [43] A. T. Liu, G. Zhang, A. L. Cottrill, Y. Kunai, A. Kaplan, P. Liu, V. B. Koman, M. S. Strano, Direct Electricity Generation Mediated by Molecular Interactions with Low Dimensional Carbon Materials-A Mechanistic Perspective, *ADVANCED ENERGY MATERIALS* 8 (35). doi:{10.1002/aenm.201802212}.
- [44] R. Zangi, Water confined to a slab geometry: a review of recent computer simulation studies, *Journal of Physics: Condensed Matter* 16 (45) (2004) S5371.
URL <http://stacks.iop.org/0953-8984/16/i=45/a=005>
- [45] R. Zangi, A. E. Mark, Monolayer ice, *Physical Review Letters* 91 (2) (2003) 025502. doi:10.1103/PhysRevLett.91.025502.
- [46] N. Giovambattista, P. J. Rossky, P. G. Debenedetti, Phase transitions induced by nanoconfinement in liquid water, *Physical Review Letters* 102 (5) (2009) 050603–.
URL <http://link.aps.org/doi/10.1103/PhysRevLett.102.050603>

- [47] P. Gallo, M. Rovere, Water at interfaces, *Journal of Physics: Condensed Matter* 22 (28) (2010) 280301.
URL <http://stacks.iop.org/0953-8984/22/i=28/a=280301>
- [48] K. Mochizuki, K. Koga, Solid–liquid critical behavior of water in nanopores, *Proceedings of the National Academy of Sciences* 112 (27) (2015) 8221–8226.
URL <http://www.pnas.org/content/112/27/8221>
- [49] F. Corsetti, J. Zubeltzu, E. Artacho, Enhanced configurational entropy in high-density nanoconfined bilayer ice, *Physical review letters* 116 (8) (2016) 085901.
- [50] J. Chen, G. Schusteritsch, C. J. Pickard, C. G. Salzmann, A. Michaelides, Two dimensional ice from first principles: Structures and phase transitions, *Phys. Rev. Lett.* 116 (2016) 025501. doi:10.1103/PhysRevLett.116.025501.
URL <https://link.aps.org/doi/10.1103/PhysRevLett.116.025501>
- [51] T. Roman, A. Groß, Polymorphism of water in two dimensions, *The Journal of Physical Chemistry C* 120 (25) (2016) 13649–13655. doi:10.1021/acs.jpcc.6b05435.
URL <https://doi.org/10.1021/acs.jpcc.6b05435>
- [52] L. Ruiz Pestana, L. E. Felberg, T. Head-Gordon, Coexistence of multilayered phases of confined water: The importance of flexible confining surfaces, *ACS Nano* 12 (1) (2018) 448–454. doi:10.1021/acsnano.7b06805.
URL <https://doi.org/10.1021/acsnano.7b06805>
- [53] M. Raju, A. van Duin, M. Ihme, Phase transitions of ordered ice in graphene nanocapillaries and carbon nanotubes, *Scientific Reports* 8 (1) (2018) 3851. doi:10.1038/s41598-018-22201-3.
URL <https://doi.org/10.1038/s41598-018-22201-3>

- [54] M. Abbaspour, H. Akbarzadeh, S. Salemi, E. Jalalitalab, Density-dependent phase transition in nano-confinement water using molecular dynamics simulation, *Journal of Molecular Liquids* 250 (2018) 26–34. doi:<https://doi.org/10.1016/j.molliq.2017.11.162>.
URL <https://www.sciencedirect.com/science/article/pii/S0167732217348298>
- [55] J. Engstler, N. Giovambattista, Comparative study of the effects of temperature and pressure on the water-mediated interactions between apolar nanoscale solutes, *The Journal of Physical Chemistry B* 123 (5) (2019) 1116–1128. doi:[10.1021/acs.jpccb.8b10296](https://doi.org/10.1021/acs.jpccb.8b10296).
URL <https://doi.org/10.1021/acs.jpccb.8b10296>
- [56] G. Algara-Siller, O. Lehtinen, F. C. Wang, R. R. Nair, U. Kaiser, H. A. Wu, A. K. Geim, I. V. Grigorieva, Square ice in graphene nanocapillaries, *Nature* 519 (7544) (2015) 443–445.
URL <http://dx.doi.org/10.1038/nature14295>
- [57] A. Calò, N. Domingo, S. Santos, A. Verdaguer, Revealing water films structure from force reconstruction in dynamic afm, *The Journal of Physical Chemistry C* 119 (15) (2015) 8258–8265.
- [58] T. Daio, T. Bayer, T. Ikuta, T. Nishiyama, K. Takahashi, Y. Takata, K. Sasaki, S. Matthew Lyth, In-situ esem and eels observation of water uptake and ice formation in multilayer graphene oxide, *Scientific Reports* 5 (2015) 11807 EP –.
URL <http://dx.doi.org/10.1038/srep11807>
- [59] S. Rouzière, P. Launois, A. M. Benito, W. K. Maser, E. Paineau, Unravelling the hydration mechanism in a multi-layered graphene oxide paper by in-situ x-ray scattering, *Carbon* 137 (2018) 379–383. doi:<https://doi.org/10.1016/j.carbon.2018.05.043>.
URL <http://www.sciencedirect.com/science/article/pii/S0008622318305037>

- [60] P. Kumar, F. W. Starr, S. V. Buldyrev, H. E. Stanley, Effect of water-wall interaction potential on the properties of nanoconfined water, *Physical Review E* 75 (1) (2007) 011202. doi:10.1103/PhysRevE.75.011202.
URL <http://link.aps.org/abstract/PRE/v75/e011202>
- [61] G. Cicero, J. C. Grossman, E. Schwegler, F. Gygi, G. Galli, Water confined in nanotubes and between graphene sheets: A first principle study, *Journal of the American Chemical Society* 130 (6) (2008) 1871–1878. doi:10.1021/ja074418+.
- [62] M. C. Gordillo, J. Martí, Structure of water adsorbed on a single graphene sheet, *Phys. Rev. B* 78 (7) (2008) 075432. doi:10.1103/PhysRevB.78.075432.
- [63] M. C. Gordillo, J. Martí, Water on graphene surfaces, *Journal of Physics: Condensed Matter* 22 (28) (2010) 284111.
URL <http://stacks.iop.org/0953-8984/22/i=28/a=284111>
- [64] D. W. Boukhvalov, M. I. Katsnelson, Y.-W. Son, Origin of anomalous water permeation through graphene oxide membrane, *Nano Letters* 13 (8) (2013) 3930–3935. doi:10.1021/nl4020292.
URL <http://dx.doi.org/10.1021/nl4020292>
- [65] M. Zhao, X. Yang, Segregation structures and miscellaneous diffusions for ethanol/water mixtures in graphene-based nanoscale pores, *The Journal of Physical Chemistry C* 119 (37) (2015) 21664–21673. doi:10.1021/acs.jpcc.5b03307.
URL <http://dx.doi.org/10.1021/acs.jpcc.5b03307>
- [66] F. Mozaffari, A molecular dynamics simulation study of the effect of water-graphene interaction on the properties of confined water, *Molecular Simulation* 42 (17) (2016) 1475–1484. doi:10.1080/08927022.2016.1204659.
URL <http://dx.doi.org/10.1080/08927022.2016.1204659>

- [67] S. Jiao, Z. Xu, Non-continuum intercalated water diffusion explains fast permeation through graphene oxide membranes, *ACS Nano* 11 (11) (2017) 11152–11161. doi:10.1021/acsnano.7b05419.
URL <https://doi.org/10.1021/acsnano.7b05419>
- [68] S. Chakraborty, H. Kumar, C. Dasgupta, P. K. Maiti, Confined water: Structure, dynamics, and thermodynamics, *Accounts of Chemical Research* 50 (9) (2017) 2139–2146. doi:10.1021/acs.accounts.6b00617.
URL <https://doi.org/10.1021/acs.accounts.6b00617>
- [69] M. Neek-Amal, A. Lohrasebi, M. Mousaei, F. Shayeganfar, B. Radha, F. M. Peeters, Fast water flow through graphene nanocapillaries: A continuum model approach involving the microscopic structure of confined water, *Applied Physics Letters* 113 (8) (2018) 083101. doi:10.1063/1.5037992.
URL <https://doi.org/10.1063/1.5037992>
- [70] R. K. Joshi, P. Carbone, F. C. Wang, V. G. Kravets, Y. Su, I. V. Grigorieva, H. A. Wu, A. K. Geim, R. R. Nair, Precise and ultrafast molecular sieving through graphene oxide membranes, *Science* 343 (6172) (2014) 752–754.
URL <http://www.sciencemag.org/content/343/6172/752>
- [71] K. G. Zhou, K. S. Vasu, C. T. Cherian, M. Neek-Amal, J. C. Zhang, H. Ghorbanfekr-Kalashami, K. Huang, O. P. Marshall, V. G. Kravets, J. Abraham, Y. Su, A. N. Grigorenko, A. Pratt, A. K. Geim, F. M. Peeters, K. S. Novoselov, R. R. Nair, Electrically controlled water permeation through graphene oxide membranes, *Nature* 559 (7713) (2018) 236–240. doi:10.1038/s41586-018-0292-y.
URL <https://doi.org/10.1038/s41586-018-0292-y>
- [72] T. Iiyama, K. Nishikawa, T. Otowa, K. Kaneko, An ordered water molecular assembly structure in a slit-shaped carbon nanospace, *The Journal of Physical Chemistry* 99 (25) (1995) 10075–10076. doi:10.1021/

j100025a004.

URL <https://doi.org/10.1021/j100025a004>

- [73] N. Choudhury, B. M. Pettitt, On the mechanism of hydrophobic association of nanoscopic solutes, *Journal of the American Chemical Society* 127 (10) (2005) 3556–3567. doi:10.1021/ja0441817.

URL <https://doi.org/10.1021/ja0441817>

- [74] N. Choudhury, B. M. Pettitt, Dynamics of water trapped between hydrophobic solutes, *The Journal of Physical Chemistry B* 109 (13) (2005) 6422–6429. doi:10.1021/jp045439i.

URL <http://dx.doi.org/10.1021/jp045439i>

- [75] J. Martí, G. Nagy, E. Guàrdia, M. C. Gordillo, Molecular dynamics simulation of liquid water confined inside graphite channels: Dielectric and dynamical properties, *The Journal of Physical Chemistry B* 110 (47) (2006) 23987–23994. doi:10.1021/jp0647277.

URL <http://dx.doi.org/10.1021/jp0647277>

- [76] N. Giovambattista, P. J. Rossky, P. G. Debenedetti, Effect of pressure on the phase behavior and structure of water confined between nanoscale hydrophobic and hydrophilic plates, *Physical Review E* 73 (4) (2006) 041604–

URL <http://link.aps.org/doi/10.1103/PhysRevE.73.041604>

- [77] G. Nagy, M. C. Gordillo, E. Guàrdia, J. Martí, Liquid water confined in carbon nanochannels at high temperatures, *The Journal of Physical Chemistry B* 111 (43) (2007) 12524–12530. doi:10.1021/jp073193m.

URL <https://doi.org/10.1021/jp073193m>

- [78] H. Mosaddeghi, S. Alavi, M. H. Kowsari, B. Najafi, Simulations of structural and dynamic anisotropy in nano-confined water between parallel graphite plates, *The Journal of Chemical Physics* 137 (18) (2012) –. doi:<http://dx.doi.org/10.1063/1.4763984>.

URL <http://scitation.aip.org/content/aip/journal/jcp/137/18/10.1063/1.4763984>

- [79] T. Sanghi, N. R. Aluru, A combined quasi-continuum/langevin equation approach to study the self-diffusion dynamics of confined fluids, *The Journal of Chemical Physics* 138 (12) (2013) 124109. [arXiv:https://doi.org/10.1063/1.4796387](https://arxiv.org/abs/1210.1063), doi:10.1063/1.4796387.

URL <https://doi.org/10.1063/1.4796387>

- [80] A. A. Chialvo, L. Vlcek, P. T. Cummings, Surface corrugation effects on the water-graphene interfacial and confinement behavior, *The Journal of Physical Chemistry C* 117 (45) (2013) 23875–23886. doi:10.1021/jp408893b.

URL <https://doi.org/10.1021/jp408893b>

- [81] J. Bordin, A. Diehl, M. C. Barbosa, Relation between flow enhancement factor and structure for core-softened fluids inside nanotubes, *The Journal of Physical Chemistry B* 117 (23) (2013) 7047–7056. doi:10.1021/jp402141f.

URL <https://doi.org/10.1021/jp402141f>

- [82] S. O. Diallo, L. Vlcek, E. Mamontov, J. K. Keum, J. Chen, J. S. Hayes, A. A. Chialvo, Translational diffusion of water inside hydrophobic carbon micropores studied by neutron spectroscopy and molecular dynamics simulation, *Phys. Rev. E* 91 (2015) 022124. doi:10.1103/PhysRevE.91.022124.

URL <https://link.aps.org/doi/10.1103/PhysRevE.91.022124>

- [83] B. H. S. Mendonça, P. Ternes, E. Salcedo, A. B. de Oliveira, M. C. Barbosa, Water diffusion in rough carbon nanotubes, *The Journal of Chemical Physics* 152 (2) (2020) 024708. doi:10.1063/1.5129394.

URL <https://doi.org/10.1063/1.5129394>

- [84] P. Hirunsit, P. B. Balbuena, Effects of confinement on water structure and dynamics: A molecular simulation study, *The Journal of Physical*

- Chemistry C 111 (4) (2007) 1709–1715. doi:10.1021/jp063718v.
URL <https://doi.org/10.1021/jp063718v>
- [85] M. Neek-Amal, F. M. Peeters, I. V. Grigorieva, A. K. Geim, Commensurability effects in viscosity of nanoconfined water, ACS Nano 10 (3) (2016) 3685–3692. doi:10.1021/acsnano.6b00187.
URL <https://doi.org/10.1021/acsnano.6b00187>
- [86] J. Engstler, N. Giovambattista, Temperature effects on water-mediated interactions at the nanoscale, The Journal of Physical Chemistry B 122 (38) (2018) 8908–8920. doi:10.1021/acs.jpcc.8b05430.
URL <https://doi.org/10.1021/acs.jpcc.8b05430>
- [87] J. Gao, W. D. Luedtke, U. Landman, Layering transitions and dynamics of confined liquid films, Physica Review Letters 79 (1997) 705–708. doi:10.1103/PhysRevLett.79.705.
URL <https://link.aps.org/doi/10.1103/PhysRevLett.79.705>
- [88] T. Samanta, R. Biswas, S. Banerjee, B. Bagchi, Study of distance dependence of hydrophobic force between two graphene-like walls and a signature of pressure induced structure formation in the confined water, The Journal of Chemical Physics 149 (4) (2018) 044502. doi:10.1063/1.5025823.
URL <https://doi.org/10.1063/1.5025823>
- [89] J. L. Abascal, C. Vega, A general purpose model for the condensed phases of water: Tip4p/2005, The Journal of chemical physics 123 (23) (2005) 234505.
- [90] U.Essmann, L.Perera, M.L.Berkowitz, T.Darden, H.Lee, L.G.Pedersen, J. Chem. Phys. 103 (1995) 8577.
- [91] B. Hess, C. Kutzner, D. Van Der Spoel, E. Lindahl, Gromacs 4: algorithms for highly efficient, load-balanced, and scalable molecular simulation, Journal of chemical theory and computation 4 (3) (2008) 435–447.

- [92] N. Giovambattista, P. J. Rossky, P. G. Debenedetti, Effect of temperature on the structure and phase behavior of water confined by hydrophobic, hydrophilic, and heterogeneous surfaces†, *The Journal of Physical Chemistry B* 113 (42) (2009) 13723–13734.
URL <http://dx.doi.org/10.1021/jp9018266>
- [93] H.J.C.Berendsen, J.P.M.Postma, W. Gunsteren, A.DiNola, J.R.Haak, *J.Phys.Chem.* 81 (1984) 3684.
- [94] S. Bernardi, B. D. Todd, D. J. Searles, Thermostating highly confined fluids, *The Journal of Chemical Physics* 132 (24) (2010) 244706. doi: 10.1063/1.3450302.
URL <https://doi.org/10.1063/1.3450302>
- [95] S. K. Kannam, B. D. Todd, J. S. Hansen, P. J. Daivis, Slip flow in graphene nanochannels, *The Journal of Chemical Physics* 135 (14) (2011) 144701. doi:10.1063/1.3648049.
URL <https://doi.org/10.1063/1.3648049>
- [96] S. Kumar Kannam, B. D. Todd, J. S. Hansen, P. J. Daivis, Slip length of water on graphene: Limitations of non-equilibrium molecular dynamics simulations, *The Journal of Chemical Physics* 136 (2) (2012) 024705. doi: 10.1063/1.3675904.
URL <https://doi.org/10.1063/1.3675904>
- [97] A. Zaragoza, M. A. González, L. Joly, I. López-Montero, M. Canales, A. Benavides, C. Valeriani, Molecular dynamics study of nanoconfined tip4p/2005 water: how confinement and temperature affect diffusion and viscosity, *Physical Chemistry Chemical Physics* 21 (25) (2019) 13653–13667.
- [98] W. Humphrey, A. Dalke, K. Schulten, VMD – Visual Molecular Dynamics, *Journal of Molecular Graphics* 14 (1996) 33–38.

- [99] B. Fábíán, M. V. Senćanski, I. N. Cvijetić, P. Jedlovszky, G. Horvai, Dynamics of the water molecules at the intrinsic liquid surface as seen from molecular dynamics simulation and identification of truly interfacial molecules analysis, *The Journal of Physical Chemistry C* 120 (16) (2016) 8578–8588. doi:10.1021/acs.jpcc.5b10370.
URL <https://doi.org/10.1021/acs.jpcc.5b10370>
- [100] C. Calero, J. Martí, E. Guàrdia, 1h nuclear spin relaxation of liquid water from molecular dynamics simulations, *The Journal of Physical Chemistry B* 119 (5) (2015) 1966–1973.
- [101] F. de los Santos, G. Franzese, Relations between the diffusion anomaly and cooperative rearranging regions in a hydrophobically nanoconfined water monolayer, *Physical Review E* 85 (1) (2012) 010602–.
URL <http://link.aps.org/doi/10.1103/PhysRevE.85.010602>
- [102] J. Gao, W. Luedtke, U. Landman, Origins of solvation forces in confined films, *The Journal of Physical Chemistry B* 101 (20) (1997) 4013–4023.
- [103] F. Varnik, J. Baschnagel, K. Binder, Molecular dynamics results on the pressure tensor of polymer films, *The Journal of Chemical Physics* 113 (10) (2000) 4444–4453.
- [104] L.-L. He, Y. Li, D.-X. Zhao, L. Yu, C.-L. Zhao, L.-N. Lu, C. Liu, Z.-Z. Yang, Structure and phase behavior of the confined water in graphene nanocapillaries studied by abeem $\sigma\pi$ polarizable force field, *The Journal of Physical Chemistry C* 123 (9) (2019) 5653–5666. doi:10.1021/acs.jpcc.8b09840.
URL <https://doi.org/10.1021/acs.jpcc.8b09840>
- [105] K. Xu, P. Cao, J. R. Heath, Graphene visualizes the first water adlayers on mica at ambient conditions, *Science* 329 (5996) (2010) 1188–1191.
- [106] S. Santos, A. Verdaguer, Imaging water thin films in ambient conditions using atomic force microscopy, *Materials* 9 (3) (2016) 182.

- [107] M. H. Köhler, J. R. Bordin, L. B. da Silva, M. C. Barbosa, Breakdown of the stokes–einstein water transport through narrow hydrophobic nanotubes, *Physical Chemistry Chemical Physics* 19 (20) (2017) 12921–12927.